Original Article

A Musculoskeletal Model for Estimating Hip Contact Pressure During Walking

Brecca M. M. Gaffney,[1,2] Spencer T. Williams,[3] Jocelyn N. Todd,[4] Jeffrey A. Weiss,[4,5,6] and Michael D. Harris [7,8,9]

[1]Department of Mechanical Engineering, University of Colorado Denver, Denver, CO, USA; [2]Center of Bioengineering, University of Colorado Anschutz Medical Campus, Aurora, CO, USA; [3]Department of Biomedical Engineering, Washington University in St. Louis, St. Louis, MO, USA; [4]Biomedical Engineering, University of Utah, Salt Lake City, UT, USA; [5]Department of Orthopaedics, University of Utah, Salt Lake City, UT, USA; [6]Scientific Computing and Imaging Institute, University of Utah, Salt Lake City, UT, USA; [7]Program in Physical Therapy, Washington University in St. Louis School of Medicine, 4444 Forest Park Ave., Suite 1101, St. Louis, MO 63108, USA; [8]Department of Orthopaedic Surgery, Washington University in St. Louis School of Medicine, St. Louis, MO, USA; and [9]Department of Mechanical Engineering and Materials Science, Washington University in St. Louis, St. Louis, MO, USA

Associate Editor Stefan M. Duma oversaw the review of this article.

Abstract—Cartilage contact pressures are major factors in osteoarthritis etiology and are commonly estimated using finite element analysis (FEA). FEA models often include subject-specific joint geometry, but lack subject-specific joint kinematics and muscle forces. Musculoskeletal models use subject-specific kinematics and muscle forces but often lack methods for estimating cartilage contact pressures. Our objective was to adapt an elastic foundation (EF) contact model within OpenSim software to predict hip cartilage contact pressures and compare results to validated FEA models. EF and FEA models were built for five subjects. In the EF models, kinematics and muscle forces were applied and pressure was calculated as a function of cartilage overlap depth. Cartilage material properties were perturbed to find the best match to pressures from FEA. EF models with elastic modulus = 15 MPa and Poisson's ratio = 0.475 yielded results most comparable to FEA, with peak pressure differences of 4.34 ± 1.98 MPa (% difference = 39.96 ± 24.64) and contact area differences of 3.73 ± 2.92% (% difference = 13.4 ± 11.3). Peak pressure location matched between FEA and EF for 3 of 5 subjects, thus we do not recommend this model if the location of peak contact pressure is critically important to the research question. Contact area magnitudes and patterns matched reasonably between FEA and EF, suggesting that this model may be useful for questions related to those variables, especially if researchers desire inclusion of subject-specific geometry, kinematics, muscle forces, and dynamic motion in a computationally efficient framework.

INTRODUCTION

Hip osteoarthritis is one of the most debilitating and prevalent musculoskeletal diseases in the United States, costing an estimated $100 billion annually, and is expected to affect over 41 million adults by 2030.[30] Altered intra-articular mechanics are known mechanical contributors to the development, progression, and severity of hip osteoarthritis,[19] particularly in populations with structural hip deformities (e.g., acetabular dysplasia[16]). As such, understanding the mechanisms of how intra-articular cartilage mechanics are altered is imperative for understanding the etiology of osteoarthritis.

Altered cartilage contact pressure has previously been established as a predictor of articular cartilage damage, yet cannot be measured directly in-vivo.[32] As a surrogate, hip cartilage contact pressure is most commonly estimated in-silico using finite element analysis (FEA)[20,22] or discrete element analysis (DEA).[37] These types of models, however, have two primary limitations that impede their clinical utility.

Address correspondence to Michael D. Harris, Program in Physical Therapy, Washington University in St. Louis School of Medicine, 4444 Forest Park Ave., Suite 1101, St. Louis, MO 63108, USA. Electronic mail: harrismi@wustl.edu

First, the computational burden often remains too large to solve for highly dynamic activities. Therefore, cartilage contact mechanics estimated using FEA models are most commonly limited to singular points within a task, which likely are not indicative of more time-varying loads experienced during dynamic motion. Second, FEA or DEA models do not simultaneously integrate the roles of complex patient-specific joint geometry, joint kinematics, and muscle function. Specific to the hip, muscle forces are the greatest contributors to joint loading.[12] Therefore, establishing a modeling platform that can estimate cartilage mechanics while simultaneously incorporating subject-specific geometry, movements, and muscle forces can significantly advance our understanding of the etiology of hip osteoarthritis.

Elastic foundation (EF) models are more computationally efficient than FEA or DEA by computing cartilage contact pressure as a function of overlap depth between two intersecting cartilage layers.[9] Recently, a tool was developed to further increase the computational efficiency of an EF model by measuring overlap depth using ray-casting oriented bounding boxes to estimate knee cartilage contact pressure during dynamic full-body movement simulations.[33] A notable advantage of this tool was that it was developed within the OpenSim musculoskeletal platform,[13] which allows the estimation of muscle forces during dynamic activities. Using this platform, subject-specific geometry, joint kinematics, and muscle function were simultaneously considered in the estimation of knee cartilage contact pressures during walking.[29,34] However, this type of model has not yet been developed or applied to the hip. An EF model of the hip that incorporates subject-specific bony geometry, muscle forces, and resulting cartilage contact pressures could provide rapid estimation of the multi-factorial contributions to abnormal intra-articular hip mechanics during a variety of activities.

Accordingly, the objective of this study was to adapt the EF contact model within OpenSim to predict cartilage contact pressures in the hip, and then compare pressure results to validated FEA models.

MATERIALS AND METHODS

Subjects and Experimental Data

With Institutional Review Board approval and informed consent, CT arthrograms and whole-body motion capture data during walking were collected from five healthy subjects (Table 1) as reported previously.[20] CT images included the pelvis and proximal femurs and have been made publicly available (https://

TABLE 1. Subject demographics

Subject	Sex	Age (years)	BMI (kg/m^3)
Sub1	F	31	22.3
Sub2	F	21	18.9
Sub3	M	27	28.1
Sub4	F	29	18.2
Sub5	F	21	29.4
Mean $\pm$ 1 S.D	–	25.8 $\pm$ 4.6	23.4 $\pm$ 5.2

mrl.sci.utah.edu/software/hip-data/). To improve segmentation accuracy, CT arthrogram images were up-sampled with a 0.3-mm slice thickness.[20] Three-dimensional reconstructions of the pelvis, and bilateral proximal femurs, as well as the acetabular and femoral cartilage for the hip that received the CT arthrogram (i.e., index hip), were generated using Amira (v5.3, Visage Imaging, San Diego, CA). Segmentation was performed using previously validated semi-automated threshold settings.[4,8]

As reported previously, each subject was instrumented with 21 reflective markers, based on a modified Helen-Hayes marker set, to obtain whole-body kinematics recorded from 10 infrared cameras during overground walking at a self-selected pace on a 10-m walkway (100 Hz sampling frequency) (Vicon, Oxford, UK).[21] Ground reaction forces were simultaneously collected from 4 embedded force platforms (1000 Hz sampling frequency) (AMTI, Watertown, MA). Kinematic and kinetic data were filtered with a 4th-order Butterworth filter (6 and 20 Hz cutoff frequencies, respectively).

Musculoskeletal Contact Model

A generic OpenSim musculoskeletal model (26 degrees-of-freedom and 96 muscle–tendon actuators) specific to the hip (available at https://simtk.org/home/hip_muscles/) was personalized for each subject. Personalization of the models was previously described in detail,[21] but main changes include: (1) substituting the pelvis and femur geometries in place of the existing generic OpenSim geometry, (2) including subject-specific bilateral hip joint centers, and (3) customization of muscle paths to the subject-specific geometry. For the current study, we also included the subject-specific articular cartilage geometry for the acetabulum and femur of the index hip.

The index hip joint in each model was modified from the traditional ball and socket to include 6 degrees-of-freedom (three rotation, three translation). Joint kinematics and muscle forces were computed within the Concurrent Optimization of Muscle Activations and Kinematics (COMAK) framework.[11]
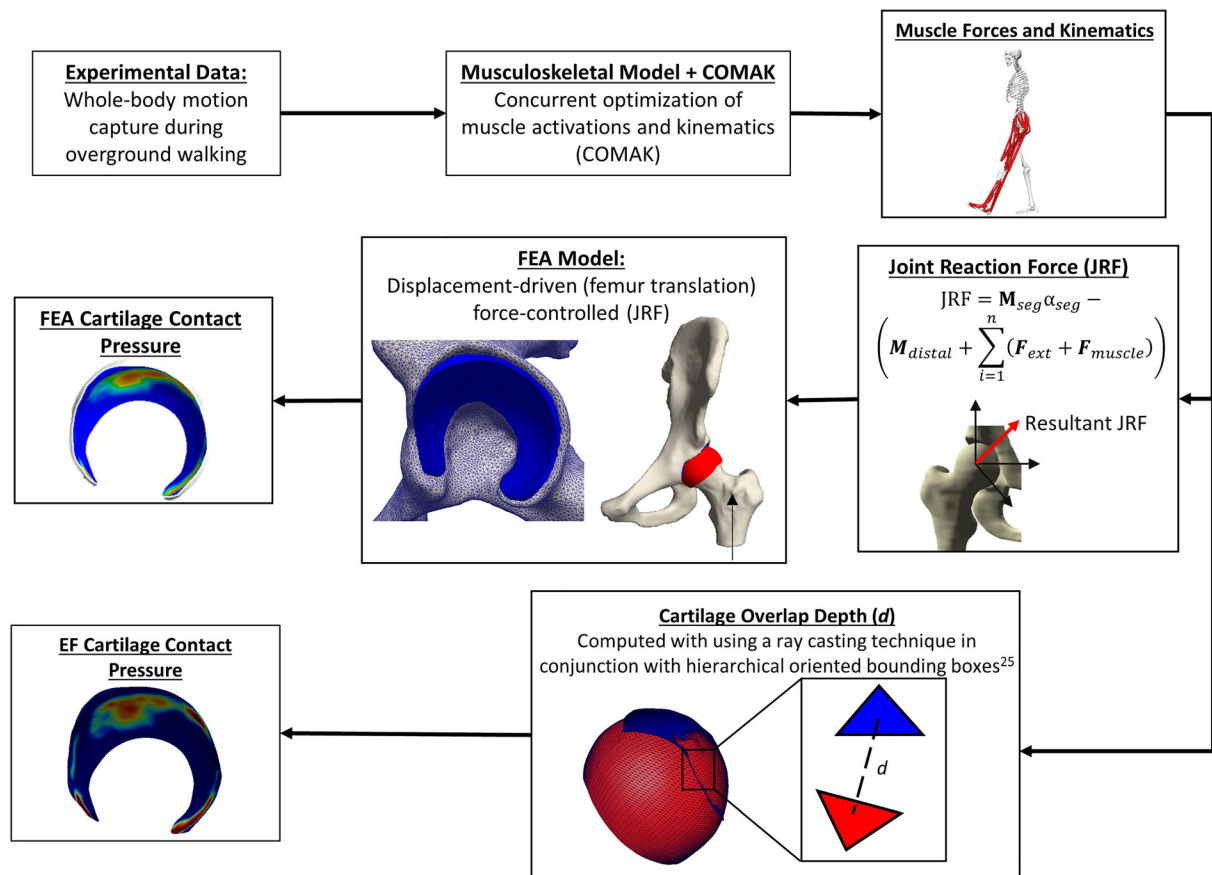
FIGURE 1. Modeling workflow that utilized subject-specific in-vivo motion data collected from each subject during walking to compute cartilage contact pressure in the elastic foundation (EF) and finite element (FEA) models.

COMAK assigns a set of primary coordinates that are readily measured using motion capture and a set of secondary coordinates that cannot be measured with confidence. In our study, primary kinematics coordinates included lumbar extension, hip flexion, hip abduction, knee flexion, and ankle plantar flexion while secondary kinematics coordinates included hip rotation and three degree-of-freedom hip translations. At each time step, the prescribed primary kinematics were set to the measured values determined using inverse kinematics. The COMAK framework then predicted secondary kinematics, muscle forces, and articular contact pressures (described below) that were dynamically consistent with the primary kinematics and ground reaction forces. Specifically, COMAK optimized secondary kinematics and muscle activations to generate the measured primary coordinates' accelerations and simultaneously minimize a cost function (J) (Eq. 1) based on the sum of squared muscle activations (a_i), as previously described.[11,33]

$$J = \sum_{i=1}^{nMuscles} W_i * V_i * a_i^2 \qquad (1)$$

where W_i is a weighting term and V_i is the muscle volume.[11] W_i was set to 1 for all muscles. Within this kinematic solution, hip joint translations were filtered *post-hoc* using a 4th-order low pass filter (4 Hz cutoff frequency) due to their high sensitivity to input noise from the experimental data.

Hip contact was integrated into this model by first representing the articulating surfaces of the femur and acetabular cartilage as single layers using triangulated surface meshes. The acetabular and femoral cartilage layers contained 10,000 and 16,200 elements, respectively, and were derived by converting the contact surface of meshes used in the validated FE models (Sect. Finite Element Model) into triangular elements. Cartilage contact pressure was calculated using the Joint Articular Mechanics (JAM) OpenSim plugin (available at https://simtk.org/projects/opensim-jam). Overlap depth was computed using a ray casting technique in conjunction with hierarchical oriented bounding boxes (Fig. 1).[33] Specifically, as the kinematic and muscle force solutions from COMAK were applied to the model, the cartilage meshes overlapped and the magnitude of overlap depth was used to

TABLE 2. Material properties (Poisson's ratio and elastic modulus) tested within the elastic foundation model.

	Elastic Modulus (E) (MPa)											
	5	6	7	8	9	10	11	11.85	12	13	14	15
Poisson's Ratio (v)												
0.42									32			
0.43												
0.44												
0.45	34							4				
0.46												
0.47		12										
0.475												19

A design of experiments was performed to determine which combination of material properties resulted in the lowest error compared to FEA. Shading indicates which combinations of material properties were tested. Numbered boxes indicate previous studies from which specific material properties were referenced.

determine cartilage contact pressure according to the elastic foundation (EF) theory (Eq. 2):[9]

$$p = \frac{(1-v)E}{(1+v)(1-2v)} \ln\left(1 - \frac{d}{h}\right) \quad (2)$$

where v is the Poisson's ratio, E is the elastic modulus, d is the overlap depth between corresponding cartilage elements, and h is the cartilage thickness.

Because contact pressures are inherently dependent on material properties, it is important to establish the most appropriate material properties for the purpose of the model. However, cartilage material property definitions have been highly variable in prior EF models. To determine the most appropriate cartilage material properties for this model, we identified the range of properties used within the EF hip contact model literature (($E = 5$ MPa and $v = 0.45$[33]; $E = 6$ MPa and $v = 0.47$[10]; $E = 11.85$ and $v = 0.45$[2]; $E = 12$ MPa and $v = 0.42$[31]; $E = 15$ and $v = 0.475$[18])) and performed a design of experiments within this range to determine which combination of material properties minimized the cartilage contact errors compared to the 'gold standard' FEA model (Sects. FiniteElement Model, Comparison to Gold-Standard FEA). Within this space, 16 total models were generated for each person, resulting in a total of 80 subject-specific models (Table 2).

Muscle forces estimated from the EF contact model were used to calculate the total muscle-driven hip joint reaction force (JRF).[35] The hip JRF was then used to drive the FEA model (Fig. 1, Sect. Finite Element Model).

Finite Element Model

A previously developed and validated FEA model[20] was used as the gold-standard for evaluation of contact pressures from the EF model. Prior validation of the FEA methods involved comparison between modeled and in vitro contact stresses measured at different points of the gait cycle. The validation process included determining the constitutive models, material properties, segmentation methods, mesh densities, and boundary conditions used in the current study.[6,7,20] The FEA model used cortical bone surfaces discretized with shell elements and modeled as a homogenous, isotropic material ($E = 17$ GPa and $v = 0.29$). Acetabular and femoral cartilage were represented with 15,000 and 24,300 hexahedral elements, respectively, and modeled as a homogenous, isotropic, nearly incompressible ($v = 0.495$), neo-Hookean hyperelastic material with shear modulus $G = 13.6$ MPa and bulk modulus $K = 1359$ MPa.

The FEA model was positioned according to the COMAK kinematics computed from the experimental data (Fig. 1, Sect. Subjects and Experimental Data). A displacement-driven force-controlled approach was used by translating the femur to load the femur/acetabulum contact interface until the target contact force, which was the maximum hip JRF calculated from the musculoskeletal model, was achieved.

Comparison to Gold-Standard FEA

For each EF model, cartilage contact was computed throughout the gait cycle (heel strike to heel strike). At the point of maximum hip JRF, the total contact area (mm^3) and peak contact pressure (MPa) were identified. Similarly, the total contact area and peak contact pressure at the target contact force was computed from each FEA model. Differences between the EF and FEA models were calculated as raw differences (Eq. 3), as well as percent differences (Eq. 4) to normalize
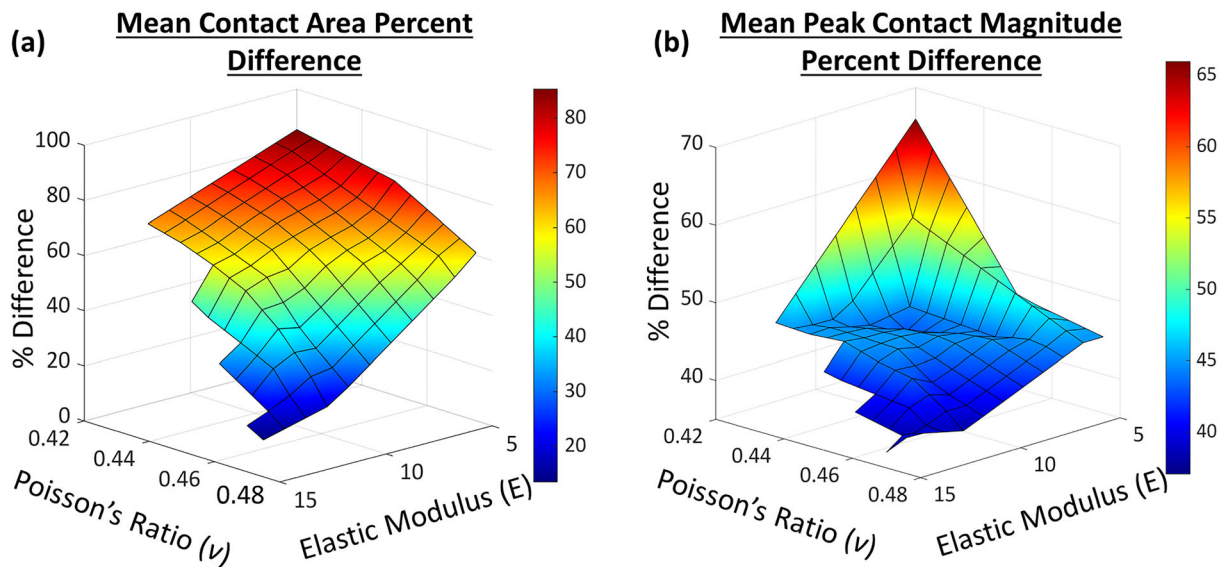
(a)

(b)

FIGURE 2. Mean percent difference across all five subject models in (a) contact area and (b) peak contact pressure magnitude between FEA and EF models across all material properties specified in Table 1. Heat map represents % difference magnitudes.

TABLE 3. Raw and percent differences between contact area and peak contact pressure magnitude at the maximum hip joint reaction forces between the FEA model and the EF model with material properties *E* = 15 MPa and *v* = 0.475

	Peak pressure (MPa)				Contact area (%)			
	FEA	EF	Raw Diff	% Diff	FEA	EF	Raw Diff	% Diff
Sub1	15.58	9.52	6.06	48.29	22.32	30.81	8.49	31.96
Sub2	13.54	15.65	2.11	14.46	25.08	28.07	2.99	11.25
Sub3	11.98	5.23	6.75	78.44	26.76	23.28	3.48	13.91
Sub4	12.34	9.15	3.19	29.69	27.36	26.89	0.47	1.73
Sub5	14.2	10.61	3.59	28.94	36.72	39.92	3.2	8.35
Mean ± 1 S.D			4.34 ± 1.98	39.96 ± 24.64			3.73 ± 2.92	13.4 ± 11.3

variations that occur due to inter-subject differences in JRF magnitudes. Overall contact pattern differences and the location of peak contact pressure were qualitatively compared.

$$RawDiff = |FEA - EF| \qquad (3)$$

$$\%Diff = 100 \times \frac{|FEA - EF|}{\left[\frac{(FEA+EF)}{2}\right]} \qquad (4)$$

RESULTS

Contact Area

Mean contact area percent differences between FEA and EF ranged between 13.4 and 85.3% (Fig. 2). Averaged across the five subjects, the lowest overall percent difference between the FEA and EF models was 13.4 ± 11.3%, which occurred in the model with material properties *E* = 15 MPa and *v* = 0.475 (Fig. 2a, Table 3).

Peak Contact Pressure

Mean peak contact pressure percent differences ranged between 37.0 and 66.0% (Fig. 2a). Averaged across the five subjects, the lowest overall difference between the FEA and EF models was 37.04 ± 28.67%, which occurred in the model with material properties *E* = 15 MPa and *v* = 0.47 (Fig. 2b, Table 3).

Location of Peak Contact Pressure and Contact Pressure Patterns

Across all five subjects, EF contact patterns generally qualitatively corresponded to the FEA models better with higher elastic modulus (i.e., stiffer) and
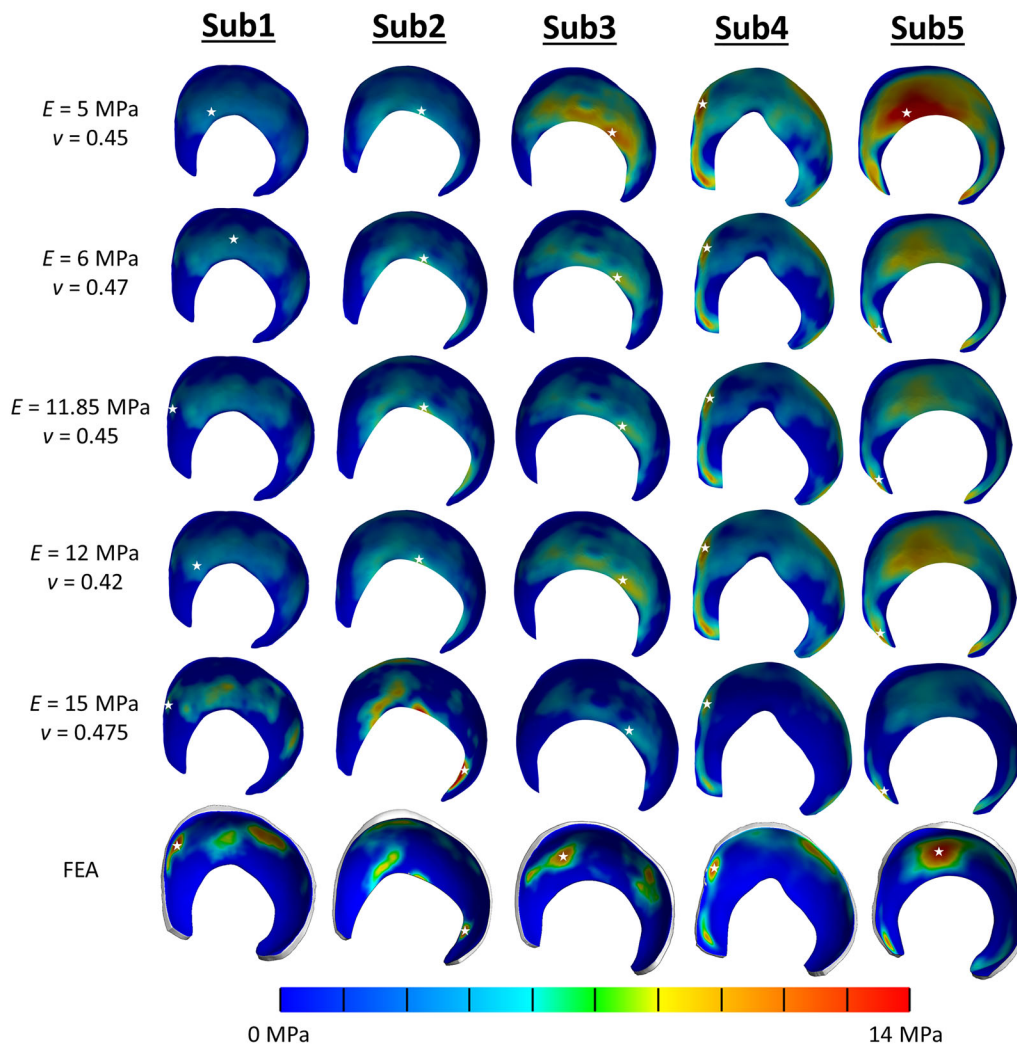
FIGURE 3. Contact pressures on the acetabular cartilage for each subject during walking calculated using the gold-standard FEA (bottom row) and EF models with varying material properties. Left is anterior. White stars indicate location of peak contact pressure.

higher Poisson's ratio (i.e., more transversely deformable) material properties (Fig. 3). With the material properties of $E = 15$ MPa and $v = 0.475$, there was excellent correspondence in the location of peak contact pressure between the FEA and EF models in three subjects (Sub1, Sub2, and Sub4) (Fig. 3).

Optimal Material Properties: E = 15 MPa and v = 0.475

Collectively considering percent differences of contact area, magnitude of the peak contact pressure, as well as the qualitative assessment of the location of peak pressure, the material properties $E = 15$ MPa and $v = 0.475$ in the EF model produced results nearest the gold-standard FEA models.

DISCUSSION

The objective of this investigation was to develop an EF musculoskeletal hip contact model and compare its prediction of cartilage contact pressures to a previously validated FEA model. Qualitatively, the contact patterns showed promising agreement between the EF and the FEA models. Quantitatively, contact areas between the EF and FEA models were also similar. Maximum contact pressure magnitudes differed more substantially between models, with the EF model generally under-predicting the magnitude of contact pressure. As part of model development, we also sought to establish the most appropriate cartilage material properties for this specific model. Considering all models, the mean error of total contact area, peak contact pressure, and overall contact pressure distribution decreased with larger elastic modulus and Poisson's ratio. Among the

BMES BIOMEDICAL ENGINEERING SOCIETY

tested combinations of material properties, the EF model with $E = 15$ MPa and $v = 0.475$ was the best match to the FEA model.

Contact area was the metric with best agreement between EF and FEA models. Because contact area was reported as a percent of the total articulating acetabular surface it is already a normalized value. Thus, interpretation of contact area results may be most meaningful by examining raw differences between EF and FEA. Among the five subjects, raw differences in contact area were less than ten percent, being less than four percent for all but one subject. This magnitude of raw differences between a novel model and an FEA gold standard is consistent with prior hip studies performing similar validation techniques.[2,24]

The peak contact pressure magnitude varied in agreement between the EF and FEA models among subjects. Raw differences in peak pressure magnitude averaged 4.34 MPa between EF and FEA models, which is in agreement with prior hip studies using similar validation techniques.[2,24] As a percent difference, the contrast in peak pressures between EF and FEA averaged approximately 40%, which we attribute to be a combination of the inability of the EF model to account for both the Poisson effect and viscoelastic material properties of the cartilage. Inherently, cartilage loading causes transverse deformation, which will affect contact pressure estimates.[2] The percent differences in peak contact pressure magnitudes are in the range of previous investigations comparing different constitutive models.[2,24] However, depending on the research question, such as questions of differences between two patient groups, the amount of magnitude difference between EF and FEA may not be suitable. For example, a prior study estimated a difference in peak cartilage contact pressure of 3.2 MPa between symptomatic and non-symptomatic hips with femoroacetabular impingement,[28] which is less than the peak pressure errors of the current EF model. Conversely, a study of surgery for acetabular dysplasia found changes in pre-surgery to post-surgery peak pressures averaged 7 MPa, which may be detectable with the current EF model.[1] If data were available, it would be ideal to compare pressure findings from EF to FEA models in specific pathological groups prior to more broadly using the EF model for peak pressure estimation. However, because the EF model tended to under estimate contact pressure in most, but not all, of the current subjects, we do not recommend use of this model if the absolute magnitude of peak contact pressure is of critical importance to the research question.

The location of peak contact pressure in the EF model agreed well with the FEA models in three of the five subjects (Sub1, Sub2, Sub4). Incidentally, in the two subjects for which location of peak pressure did not agree (Sub3 and Sub5), each EF model had a secondary "hotspot" of high pressure that did align well with the peak location in FEA. Thus, determining the location of the peak contact pressure with this EF model should be done with caution but may be appropriate when analyses consider multiple areas of contact rather than being myopically focused on a single peak value.

Understanding cartilage contact patterns is important because regions of altered contact distribution correspond to locations of cartilage degeneration. For example, in cases of acetabular dysplasia, contact loading is more concentrated near the acetabular edge and corresponds with common locations of joint damage.[3] A primary objective of periacetabular osteotomy surgery to treat acetabular dysplasia, is to shift cartilage pressures away from the acetabular edge and increase cartilage contact area.[26] Prior modeling studies using FEA or DEA have demonstrated that periacetabular osteotomy can reduce peak contact pressures and increase contact area.[2,17] However, postsurgical changes in cartilage contact, as modeled previously, were not consistent for all patients, did not necessarily correspond to changes in patients' symptoms, and did not provide explanations for the inconsistencies. Incorporating the movement patterns and muscle forces included in the current EF model, along with contact pattern metrics, offers the potential for a more holistic assessment of joint loading.

The overall utility of the EF model is best determined by considering its strengths and weaknesses. A strength of the EF model is its inclusion of subject-specific bony geometry, joint kinematics, and muscle forces that facilitate estimation of cartilage contact pressure throughout dynamic activities. Although FEA models are considered the gold standard in cartilage loading computation, computational burden often does not allow analysis of cartilage loading across a continuum of motion. Also, with a few exceptions, FEA frameworks rarely include subject-specific muscle forces as loading conditions.[15,25] This limitation can hinder the translation of FEA models to clinical applications. The lack of subject-specific muscle forces is particularly relevant when studying populations with pre-arthritic hip disorders. These patients tend to be younger and experience symptoms during higher-demand activities when muscle forces and joint positioning play a large role in articular loading. Another strength of the EF model is how nearly it predicted contact areas and general contact patterns compared to the FEA models. While contact area cannot fully describe articular contact patterns, it is a common metric used by researchers and clinicians to quantify both pressure abnormalities and the effect of

treatment. The close agreement found with the EF model provides a level of confidence for researchers interested in contact pattern changes that may arise due to disease, injury, or clinical intervention (e.g., surgery).

Conversely, the varied agreement in peak contact pressure magnitude between the EF and FEA models is a weakness. To explain disparities between the modeling methods, it is important to recognize the differences in constitutive models that influence behavior of the simulated cartilage layers. The FEA model incorporates cartilage deformation into estimates of loading while the EF model incorporates a rigid body assumption across all bodies and uses only a mathematical estimate of cartilage deformation based on overlap depth. Thus, for research questions requiring rigorous analysis of cartilage deformation and absolute peak cartilage pressures the EF model would not be an appropriate choice. The EF model predicted peak pressures better when contact occurred near the edges of the cartilage. This behavior may be due to inaccuracies in the predicted medial–lateral translation of the femur. The COMAK framework predicts secondary kinematics, such as hip translations, based on primary kinematics, such as hip flexion.[11] There is not definitive published data describing hip translations as a function of hip flexion so we cannot know if the COMAK-predicted translations (albeit very small) are accurate. Also, errors inherently exist in primary kinematics due to motion and soft-tissue artifacts, which can propagate through the entire modeling process. Because subjects in the current study had healthy hips and low body-mass indexes, errors in primary kinematics may have been low, but would likely increase in overweight subjects. Overall, the efficacy of the EF model is likely to improve in future investigations with precisely stipulated translational kinematics quantified with tools such as biplanar radiography.

In addition to the general limitations of an EF model, there are limitations specific to this study that should also be considered. First, the labrum was not included in either the FEA or EF models. It has previously been shown that the acetabular labrum alters cartilage contact mechanics in specific patient populations.[23,36] Future work should explore including the labrum in this musculoskeletal EF hip contact model. Second, no ligaments were considered in the EF model. The original model used in the JAM plugin, developed by Lenhart et al. (2015), incorporated 14 knee ligaments. Although the hip capsule ligaments affect joint stability,[14,27] and may influence cartilage contact pressure, we sought to assess the EF model using a boundary and loading scheme similar to most prior hip contact models, except with the addition of muscle forces and a dynamic task. The inclusion of the hip capsule ligaments, which is much more complex than the discrete bundles within the knee, was outside the scope of our initial model validation step and will be explored in future work. Third, the EF model is only capable of computing compressive cartilage contact pressure; and as such, contact pressure was the only variable used for model validation. It is becoming increasingly apparent that cartilage delamination in certain patient populations is a product of shear and contact stresses.[5] Therefore, users should understand the model's limitations when choosing when and how to apply the current model. Finally, sex was not considered as a biological variable within this analysis. Selection of the retrospective data used for this analysis was based upon data availability, not subject demographics, but there is no reason to believe that sex had an impact on our FEA to EF comparisons.

In conclusion, we developed an EF musculoskeletal hip contact model to estimate cartilage contact mechanics during walking. A key benefit of this model is that it can estimate cartilage contact pressures while incorporating subject-specific kinematics, muscle forces, and bony geometry. The EF model estimated contact areas and general contact patterns that were similar to FEA. However, because the EF model tended to inconsistently underestimate peak contact pressure, we do not recommend its use if a single value of peak contact pressure is of critical importance to the research question. Nonetheless, the ability to estimate dynamic cartilage contact mechanics in a computationally efficient manner, while allowing this level of subject-specificity, has broad clinical impacts. For example, this model could be used to establish how cartilage mechanics are altered across varying tasks of biomechanical demand, which currently is not well understood. This information could be used to better inform targeted patient and task-specific interventions aimed at joint preservation against osteoarthritis.

BMES BIOMEDICAL ENGINEERING SOCIETY

AUTHOR CONTRIBUTIONS

Each author was fully involved in the conception and design of the study, data acquisition and analysis, manuscript preparation, and final approval of the submitted manuscript.

CONFLICT OF INTEREST

All authors declare that they have no conflict of interest.

REFERENCES

[1]Abraham, C. L., S. J. Knight, C. L. Peters, J. A. Weiss, and A. E. Anderson. Patient-specific chondrolabral contact mechanics in patients with acetabular dysplasia following treatment with periacetabular osteotomy. *Osteoarthr. Cartil.* 25:676–684, 2017.

[2]Abraham, C. L., S. A. Maas, J. A. Weiss, B. J. Ellis, C. L. Peters, and A. E. Anderson. A new discrete element analysis method for predicting hip joint contact stresses. *J. Biomech.* 46:1121–1127, 2013.

[3]Aitken, H. D., R. W. Westermann, N. I. Bartschat, A. M. Meyer, M. J. Brouillette, N. A. Glass, J. C. Clohisy, M. C. Willey, and J. E. Goetz. Chronically elevated contact stress exposure correlates with intra-articular cartilage degeneration in patients with concurrent acetabular dysplasia and femoroacetabular impingement. *J. Orthop. Res.* 2022. https://doi.org/10.1002/jor.25285.

[4]Allen, B., C. Peters, N. Brown, and A. Anderson. Acetabular cartilage thickness: accruach of three-dimensional reconstructions from multidector CT arthrograms in a cadaver study. *Radiology*. 255:544–552, 2010.

[5]Anderson, A. E. CORR Insights ®: increased hip stresses resulting from a cam deformity and decreased femoral neck-shaft angle during level walking. *Clin. Orthop. Relat. Res.* 475:1009–1012, 2017.

[6]Anderson, A. E., B. J. Ellis, S. A. Maas, C. L. Peters, and J. A. Weiss. Validation of finite element predictions of cartilage contact pressure in the human hip joint. *J. Biomech. Eng.* 130:51008, 2008.

[7]Anderson, A. E., B. J. Ellis, S. A. Maas, and J. A. Weiss. Effects of idealized joint geometry on finite element predictions of cartilage contact stresses in the hip. *J. Biomech.* 43:1351–1357, 2010.

[8]Anderson, A. E., C. L. Peters, B. D. Tuttle, and J. A. Weiss. Subject-specific finite element model of the pelvis: development, validation and sensitivity studies. *J. Biomech. Eng.* 127:364, 2005.

[9]Bei, Y., and B. J. Fregly. Multibody dynamic simulation of knee contact mechanics. *Med. Eng. Phys.* 26:777–789, 2004.

[10]Besier, T. F., G. E. Gold, G. S. Beaupré, and S. L. Delp. A modeling framework to estimate patellofemoral joint cartilage stress in vivo. *Med. Sci. Sports Exerc.* 37:1924–1930, 2005.

[11]Brandon, S. C. E., C. R. Smith, and D. G. Thelen. Simulation of soft tissue loading from observed movement dynamics. Cham: Springer International Publishing, 2017.

[12]Correa, T., K. M. Crossley, H. J. Kim, and M. G. Pandy. Contributions of individual muscles to hip joint contact force in normal walking. *J. Biomech.* 43:1618–1622, 2010.

[13]Delp, S. L., F. C. Anderson, A. S. Arnold, P. Loan, A. Habib, C. T. John, E. Guendelman, and D. G. Thelen. OpenSim: open-source software to create and analyze dynamic simulations of movement. *IEEE Trans. Biomed. Eng.* 54:1940–1950, 2007.

[14]Elkins, J. M., N. J. Stroud, M. J. Rudert, Y. Tochigi, D. R. Pedersen, B. J. Ellis, J. J. Callaghan, J. A. Weiss, and T. D. Brown. The capsule's contribution to total hip construct stability - a finite element analysis. *J. Orthop. Res.* 29:1642–1648, 2011.

[15]Esrafilian, A., L. Stenroth, M. E. Mononen, P. Tanska, J. Avela, and R. K. Korhonen. EMG-assisted muscle force driven finite element model of the knee joint with fibril-reinforced poroelastic cartilages and menisci. *Sci. Rep.* 10:1–16, 2020.

[16]Ganz, R., M. Leunig, K. Leunig-Ganz, and W. H. Harris. The etiology of osteoarthritis of the hip: An integrated mechanical concept. *Clin. Orthop. Relat. Res.* 466:264–272, 2008.

[17]Goetz, J. E., H. D. Thomas-Aitken, S. E. Sitton, R. W. Westermann, and M. C. Willey. Joint contact stress improves in dysplastic hips after periacetabular osteotomy but remains higher than in normal hips. *HIP Int.* 2021. https://doi.org/10.1177/11207000211036414.

[18]Guess, T. M., H. Liu, S. Bhashyam, and G. Thiagarajan. A multibody knee model with discrete cartilage prediction of tibio-femoral contact mechanics. *Comput. Methods Biomech. Biomed. Engin.* 16:256–270, 2013.

[19]Harris, W. H. Etiology of osteoarthritis of the hip. *Clin. Orthop. Relat. Res.* 213:20–33, 1986.

[20]Harris, M. D., A. E. Anderson, C. R. Henak, B. J. Ellis, C. L. Peters, and J. A. Weiss. Finite element prediction of cartilage contact stresses in normal human hips. *J. Orthop. Res.* 30:1133–1139, 2012.

[21]Harris, M. D., B. A. MacWilliams, K. B. Foreman, C. L. Peters, J. A. Weiss, and A. E. Anderson. Higher medially-directed joint reaction forces are a characteristic of dysplastic hips: A comparative study using subject-specific musculoskeletal models. *J. Biomech.* 54:80–87, 2017.

[22]Henak, C. R., C. L. Abraham, A. E. Anderson, S. A. Maas, B. J. Ellis, C. L. Peters, and J. A. Weiss. Patient-specific analysis of cartilage and labrum mechanics in human hips with acetabular dysplasia. *Osteoarthr. Cartil.* 22:210–217, 2014.

[23]Henak, C. R., B. J. Ellis, M. D. Harris, A. E. Anderson, C. L. Peters, and J. A. Weiss. Role of the acetabular labrum in load support across the hip joint. *J. Biomech.* 44:2201–2206, 2011.

[24]Houcke, J., E. A. Van, P. R. Audenaert, and Atkins, and A. E. Anderson,. A combined geometric morphometric and discrete element modeling approach for hip cartilage contact mechanics. *Front. Bioeng. Biotechnol.* 8:1–13, 2020.

[25]Hume, D. R., P. J. Rullkoetter, and K. B. Shelburne. ReadySim: A computational framework for building explicit finite element musculoskeletal simulations directly from motion laboratory data. *Int J Numer Meth Biomed Engng.* 2020. https://doi.org/10.1002/cnm.3396.

[26]Knight, S. J., C. L. Abraham, C. L. Peters, J. A. Weiss, and A. E. Anderson. Changes in chondrolabral mechanics, coverage, and congruency following peri-acetabular osteotomy for treatment of acetabular retroversion: A patient-specific finite element study. *J. Orthop. Res.* 35:2567–2576, 2017.

[27]Ng, K. C. G., J. R. T. Jeffers, and P. E. Beaulé. Hip joint capsular anatomy, mechanics, and surgical management. *J. Bone Jt. Surg. - Am.* 101:2141–2151, 2019.

[28]Ng, K. C. G., G. Mantovani, M. Lamontagne, M. R. Labrosse, and P. E. Beaulé. Cam FAI and smaller neck angles increase subchondral bone stresses during squatting: a finite element analysis. *Clin. Orthop. Relat. Res.* 477:1053–1063, 2019.

[29]Lenhart, R. L., J. Kaiser, C. R. Smith, and D. G. Thelen. Prediction and validation of load-dependent behavior of the tibiofemoral and patellofemoral joints during movement. *Ann. Biomed. Eng.* 43:2675–2685, 2015.

[30]Nho, S. J., S. M. Kymes, J. J. Callaghan, and D. T. Felson. The burden of hip osteoarthritis in the United States: Epidemiologic and economic considerations. *J. Am. Acad. Orthop. Surg.* 21:1–6, 2013.

[31]Russell, M. E., K. H. Shivanna, N. M. Grosland, and D. R. Pedersen. Cartilage contact pressure elevations in dysplastic hips: A chronic overload model. *J. Orthop. Surg. Res.* 1:1–11, 2006.

[32]Segal, N. A., D. D. Anderson, K. S. Iyer, J. Baker, J. C. Torner, J. A. Lynch, D. T. Felson, C. E. Lewis, and T. D. Brown. Baseline articular contact stress levels predict incident symptomatic knee osteoarthritis development in the MOST cohort. *J. Orthop. Res.* 27:1562–1568, 2009.

[33]Smith, C. R., K. W. Choi, D. Negrut, and D. G. Thelen. Efficient computation of cartilage contact pressures within dynamic simulations of movement. *Comput. Methods Biomech. Biomed. Eng. Imaging Vis.* 1163:1–8, 2016.

[34]Smith, C. R., K. Won Choi, D. Negrut, and D. G. Thelen. Efficient computation of cartilage contact pressures within dynamic simulations of movement. *Comput. Methods Biomech. Biomed. Eng. Imaging Vis.* 6:491–498, 2018.

[35]Steele, K. M., M. S. Demers, M. H. Schwartz, and S. L. Delp. Compressive tibiofemoral force during crouch gait. *Gait Posture*. 35:556–560, 2012.

[36]Todd, J. N., T. G. Maak, G. A. Ateshian, S. A. Maas, and J. A. Weiss. Hip chondrolabral mechanics during activities of daily living: Role of the labrum and interstitial fluid pressurization. *J. Biomech.* 69:113–120, 2018.

[37]Townsend, K. C., H. D. Thomas-Aitken, M. J. Rudert, A. M. Kern, M. C. Willey, D. D. Anderson, and J. E. Goetz. Discrete element analysis is a valid method for computing joint contact stress in the hip before and after acetabular fracture. *J. Biomech.* 67:9–17, 2018.

BMES BIOMEDICAL ENGINEERING SOCIETY